TRIBOLOGICAL BEHAVIOR OF COMPOSITES

The tribological behaviour of Cu4Ni and composites namely, Cu4Ni-2wt. % TiC, Cu4Ni-4wt. % TiC, Cu4Ni-6 wt. % TiC and Cu4Ni-8 wt. % TiC has been investigated in terms of the friction and dry sliding wear against the counterface of steel at different loads and speeds. The primary focus of this study is to understand the role of second phase content, normal load and speed on the wear and friction characteristics of these composites. The results have also been discussed to develop a coherent understanding of the tribological characteristics of these composites in terms of their correlation with the properties of these materials as it has emerged from this study.

5.1 RESULTS

5.1.1 Dry Sliding Friction and Wear

(a) Dry Sliding Friction

(i) Variation of coefficient of friction with sliding distance

The typical variation of coefficient of friction with sliding distance at normal load of 5 N, 10 N, 15 N and 20 N for Cu4Ni, Cu4Ni-2TiC, Cu4Ni-4TiC, Cu4Ni-6TiC and Cu4Ni-8TiC composites at a constant sliding speed of 1.25 m/s against the EN31 steel counter face have been shown in Figs.5.1 (a) to (d). The friction coefficient is observed to fluctuate and the amplitude of fluctuations is observed to increase with increasing load for all the materials investigated in the present study as evident from Figs. 5.1 (a) to (d). The range of coefficient of friction at 5 N load is 0.70 - 0.85, at 10 N load is 0.74 - 0.97, at 15 N load is 0.61- 0.98 and at 20 N load it is 0.73 - 0.93. Figures 5.2 (a) and (b) depict the typical variation of coefficient of friction with sliding distance for Cu4Ni, Cu4Ni-2TiC, Cu4Ni-4TiC, Cu4Ni-6TiC and Cu4Ni-8TiC composites at normal loads of 5 N and 20 N and a constant sliding speed of 1m/s, whereas Figs. 5.3 (a and b) show the same at a speed of 0.75 m/s. Figure 5.2 (a) shows the fluctuating trends of average coefficient of friction. One can observe a similar trend of variation in Figs. 5.2 and 5.3 as observed in

Fig. 5.1. However, the amplitude of fluctuation are found to be relatively less at a sliding sped of 0.75 m/s in comparison to those for 1.0 and 1.25 m/s as evident from a comparison of Fig. 5.1, 5.2 and 5.3.

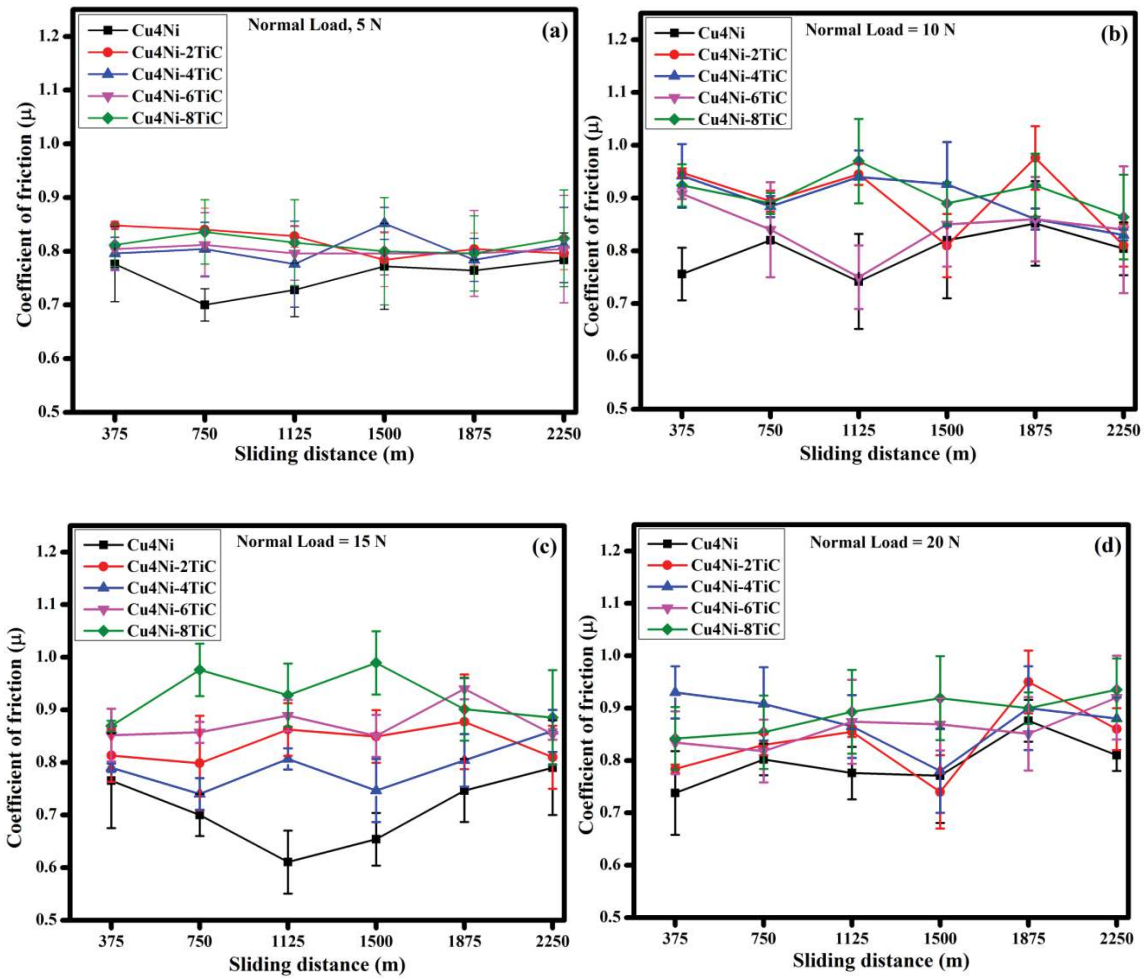

Fig.5.1: Variation of coefficient of friction with sliding distance at normal load of (a) 5 N, (b) 10N, (c) 15 N and (d) 20 N at a constant speed of 1.25 m/s.

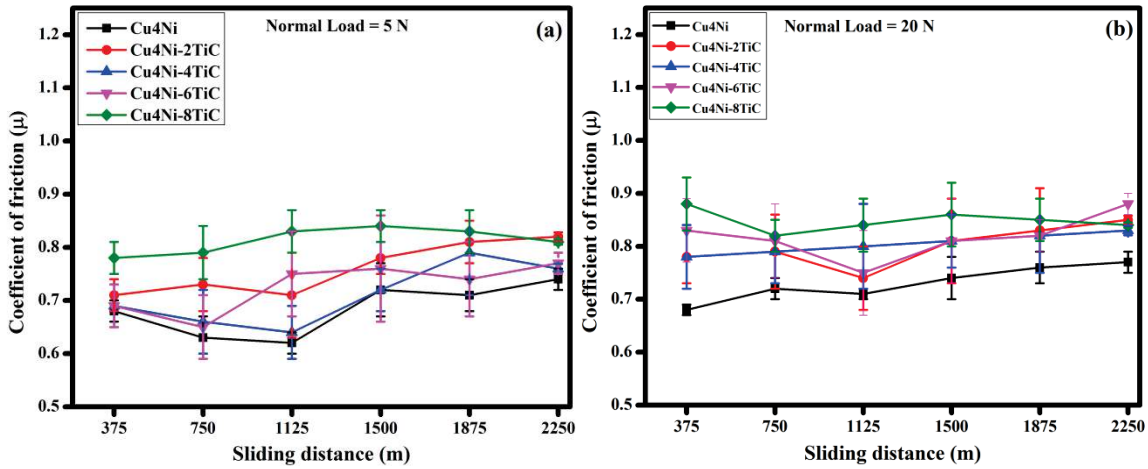

Fig.5.2: Variation of coefficient of friction with sliding distance at normal load of (a) 5 N and (d) 20 N at a constant speed of 1 m/s.

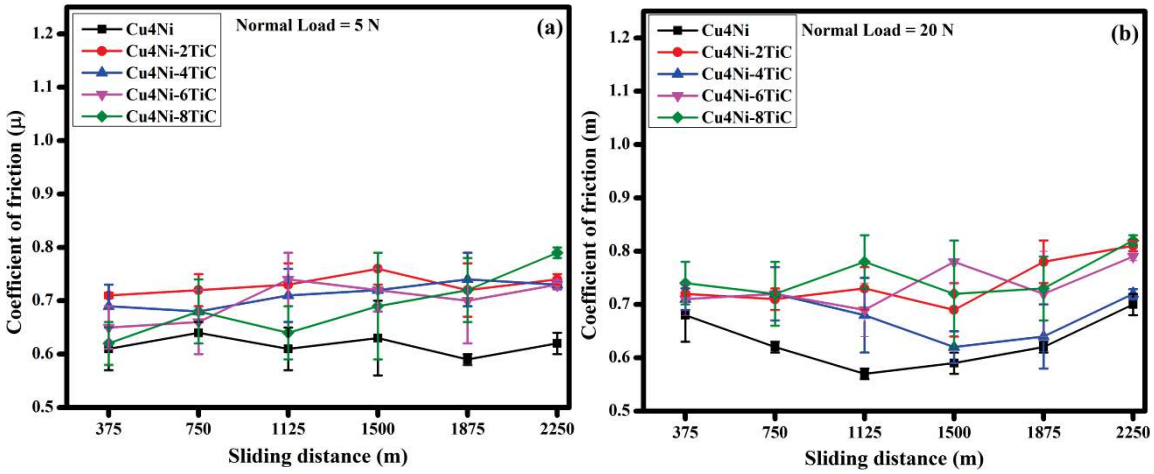

Fig.5.3: Variation of coefficient of friction with sliding distance at normal load of (a) 5 N and (d) 20 N at a constant speed of 0.75 m/s.

(ii) Variation of average coefficient of friction with normal load

Figure 5.4 shows the variation of coefficient of friction averaged over the distance slid with normal load at a constant sliding speed of 1.25 m/s for Cu4Ni, Cu4Ni-2TiC, Cu4Ni-4TiC, Cu4Ni-6TiC and Cu4Ni-8TiC composites. It is observed that average

coefficient of friction increases with increasing normal load for all the developed composites. However, for Cu4Ni matrix alloy the friction coefficient increases as the load increases from 5 to 10 N and then decreases as the load is increased to 15 N beyond which it again increases till 20 N load. It could also be observed from Fig. 5.4 that the friction coefficient shown by all the materials lie between 0.78 to 0.92. However, the friction coefficient shown by Cu4Ni alloy is the lowest and Cu4Ni-8TiC composite is the highest at all the normal loads.

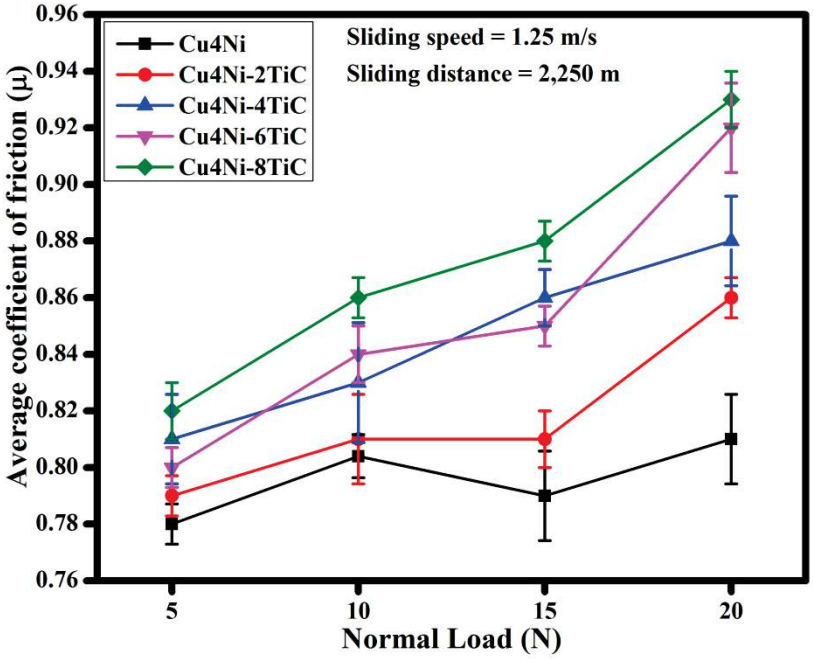

Fig.5.4: Variation of average coefficient of friction with normal load.

(iii) Variation of average coefficient of friction with sliding speed

Figure 5.5 (a) and (b) shows the variation of coefficient of friction of Cu4Ni, Cu4Ni-2TiC, Cu4Ni-4TiC, Cu4Ni-6TiC and Cu4Ni-8TiC composites with sliding speed (0.75, 1 and 1.25 m/s) at the lowest and the highest normal loads of 5 N and 20 N used in the present study. It is observed that as the sliding speed increases average coefficient of friction increases. However, Cu4Ni has shown the lowest coefficient of friction at all the speeds at both the loads whereas Cu4Ni-8TiC has shown the highest coefficient of friction as evident from Fig. 5.5 (a and b). Among the composites Cu4Ni-4TiC has

shown a consistently lower coefficient of friction at all the speeds in comparison to other composites. It can be observed that when the sliding speed is maintained for a particular load of 5 N the friction coefficient of Cu4Ni increases from 0.69 to 0.77 as the speed increases from 0.75 to 1.25 m/s. Similarly at 20 N load the coefficient of friction of Cu4Ni matrix alloy increases from 0.73 to 0.81 as sliding speed increases from 0.75 to 1.25 m/s. The coefficient of friction of composites changes marginally with increase in sliding speed at the lowest load of 5 N. However, the change in the friction coefficient with sliding speed is relatively large at the highest load of 20 N used in the present investigation as evident from a comparison of Figs. 5 (a) and 5 (b). Similar variations were seen at other loads of 10 and 15 N, hence those have not been included here. It is clear from Fig. 5.5 (a) and (b) that the average coefficient of friction of composites in all the cases is greater than matrix alloy and maximum value of coefficient of friction (COF) observed for any composite is 0.94. It can also be observed that in all the cases the coefficient of friction for both the matrix alloy as well as composites is less than 1.

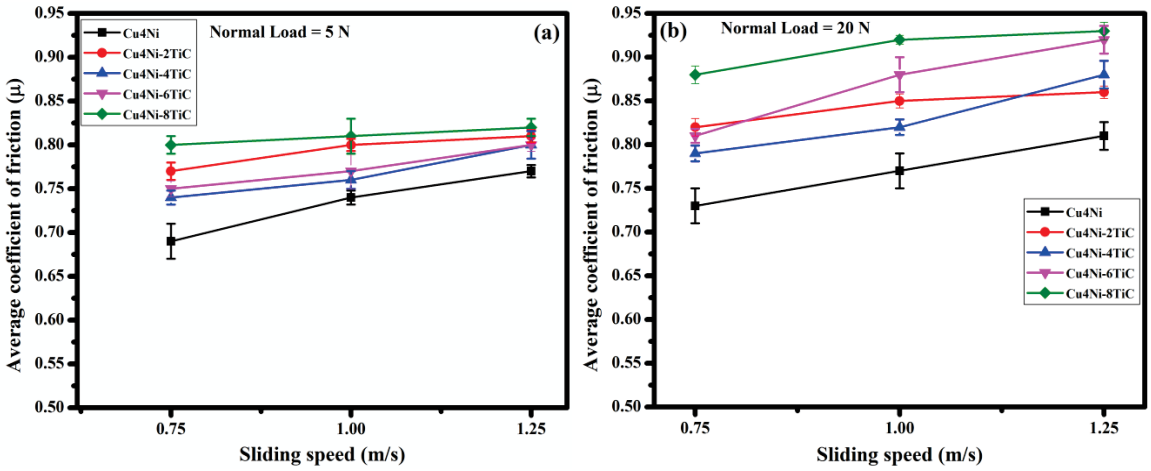

Fig.5.5: Variation of average coefficient of friction with sliding speed at normal load of (a) 5 N and (b) 20 N.

(iv) Variation of average coefficient of friction with hardness

The variation of average coefficient of friction with hardness, at loads of 5 N and 20 N for Cu4Ni, Cu4Ni-2TiC, Cu4Ni-4TiC, Cu4Ni-6TiC, and Cu4Ni-8TiC composites is shown in Fig.5.6. It can be observed from the Fig 5.6 that at a particular load say at 20 N

it increases up to Cu4Ni-4TiC and then it changes for Cu4Ni-6TiC and Cu4Ni-8TiC composites. Similar trend has been found at other loads.

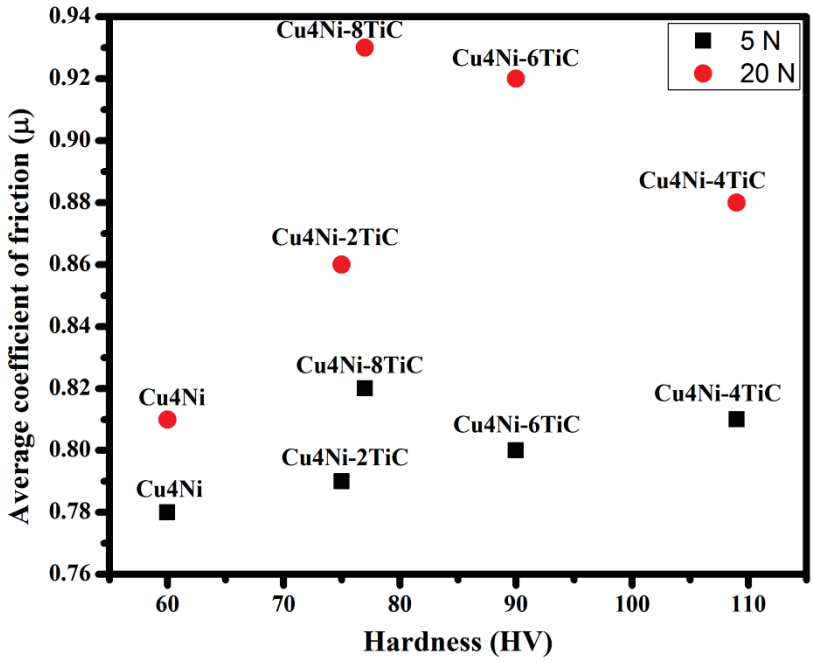

Fig.5.6: The variation of the average coefficient of friction with hardness under 5 N and 20 N for Cu4Ni, Cu4Ni-2TiC, Cu4Ni-4TiC,Cu4Ni-6TiC, and Cu4Ni-8TiC composites.

(v) Variation of average coefficient of friction with amount of TiC

Figure 5.7 illustrates the variation of average coefficient of friction with the amount of TiC at different loads for a constant sliding speed of 1.25 m/s. It is observed that average coefficient of friction increases with increase in TiC content. However, at friction coefficient is found to remain almost constant as the TiC content increase from 2 wt.% to 8 wt.% at the lowest load of 5 N whereas it is observed to increase for the loads of 10, 15 and 20 N. TiC reinforced composites have consistently shown a relatively higher coefficient of friction in comparison to the Cu4Ni matrix alloy at all the loads which could be seen from Fig. 5.7.

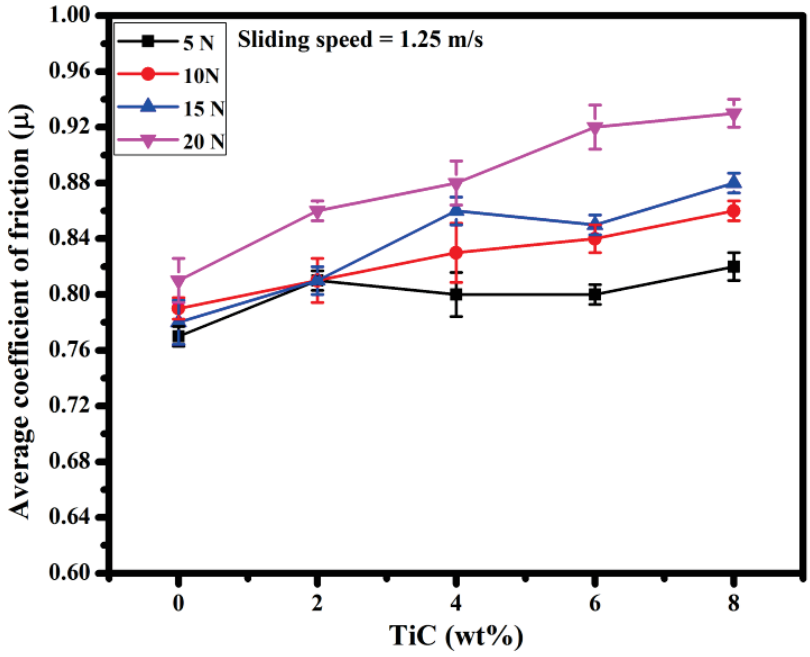

Fig.5.7: Variation of coefficient of friction with TiC reinforcement at normal load of 5 N, 10 N, 15 N and 20 N for a constant sliding speed of 1.25m/s.

(b) Dry Sliding Wear

(i) Variation of cumulative wear volume with sliding distance

Figures 5.8 (a) to (d) show the variation of cumulative volume loss with sliding distance for all the materials investigated in the present study under different loads of 5, 10, 15, 20 N and at a constant sliding speed of 1.25 m/s. The measured values of weight loss for all the specimens tested were converted into volume loss using the measured density of the specimen. The total sliding distance covered during the wear test is 2,250 m. It can be seen that the cumulative volume loss increases almost linearly with increasing sliding distance which was confirmed through curve fitting by linear least square fit. However, the data points have been shown by point by point joining in Fig. 5.8. The volume loss of matrix alloy i.e., Cu4Ni and composites namely, Cu4Ni-2TiC, Cu4Ni-4TiC, Cu4Ni-6TiC and Cu4Ni-8TiC is found to be 3.96, 2.11, 0.76, 1.79 and 2.01 mm^3 at 5N load. The volume loss at 10 N load is found to be 5.07, 2.80, 0.95, 2.12, 2.48 mm^3. The volume loss reported at load 15 N is 7.0, 4.34, 1.38, 3.83 and 4.52 mm^3 whereas the same at 20 N is 8.18, 5.49, 2.36, 4.89 and 6.02 mm^3, respectively. The cumulative volume loss shown by Cu4Ni matrix alloy is the largest among all the

materials used in the present study at all the normal loads whereas the same shown by the Cu4Ni-4TiC is the smallest as seen from Figs. 5.8 (a) to (d). The volume loss for Cu4Ni is observed to be 80.80, 81.26, 80.28 and 71.14%, higher in comparison to Cu4Ni-4TiC composite at the various load of 5, 10, 15 and 20 N.

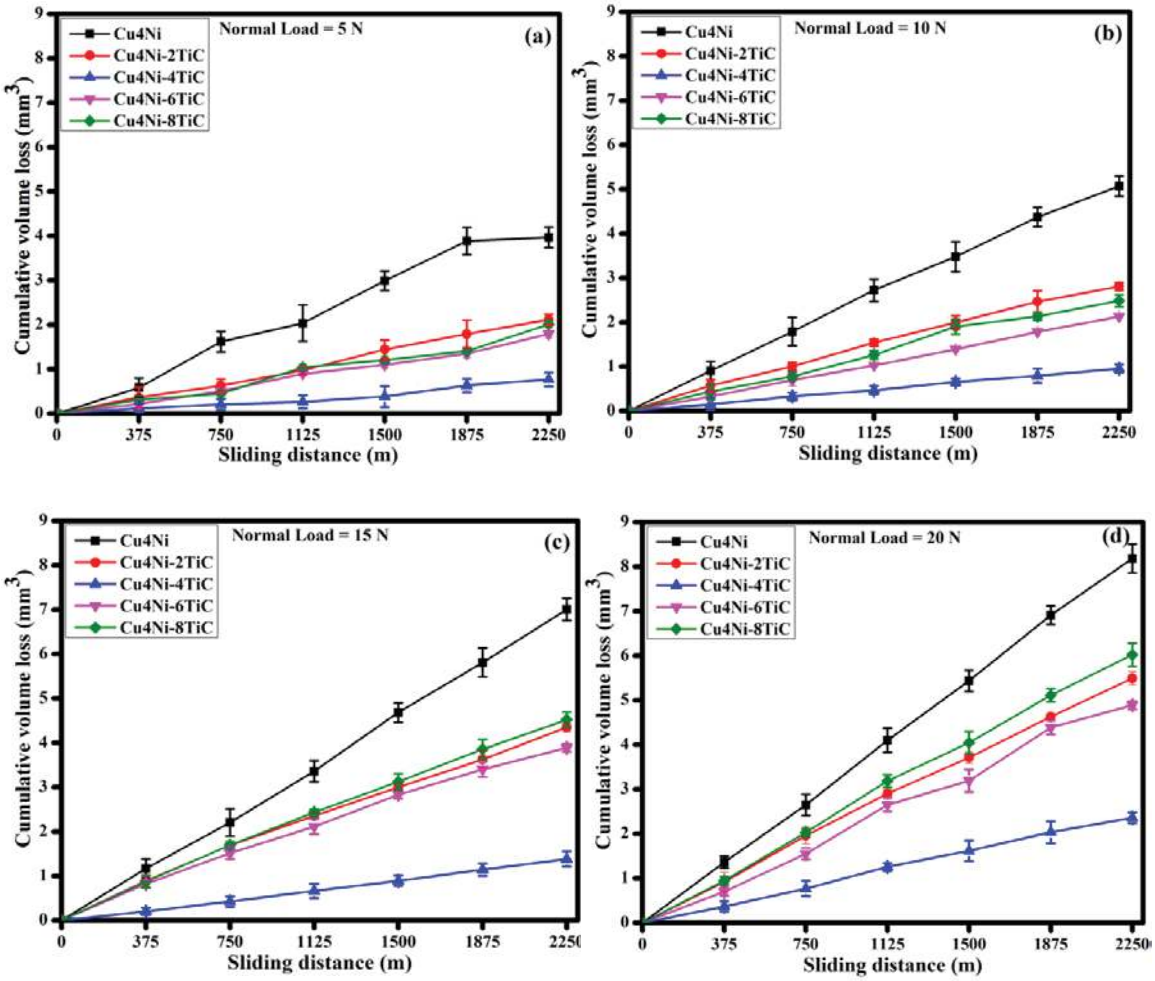

Fig.5.8: Variation of cumulative volume loss with sliding distance at normal load of (a) 5 N, (b) 10 N, (c) 15 N and (d) 20 N for a constant sliding speed of 1.25m/s.

Figures 5.9 (a) and (b) shows the variation of cumulative volume loss with sliding distance at the lowest and the highest loads of 5 N and 20 N for a constant sliding speed of 1 m/s whereas Figs.5.10 (a) and (b) depict the same for a constant sliding speed of 0.75 m/s. It can be observed that Cu4Ni has a relatively higher cumulative volume loss as compared to composites at the load of 5 N for both the speeds of 1.0 and 0.75 m/s as evident from Figs. 5.9 (a) and 5.10 (a). However, the difference between the volume loss

of Cu4Ni and composites is observed to decrease as the load is changed from 5 to 20 N which can be judged by comparison of Figs. 5.9 (a and b) and Figs. 5.10 (a and b). It could also be observed that the composite containing 4 wt.% TiC i.e. Cu4Ni-4TiC has a consistently lower cumulative volume loss among all the composites at all the normal loads for both 1.0 m/s and 0.75 m/s as evident from Fig. 5.9 and 5.10. The cumulative volume los shown by other composites namely, Cu4Ni-2TiC, Cu4Ni-6TiC and Cu4Ni-8 TiC appear to fall in the same band at the lowest load of 5 N whereas these have a marginal difference at the highest load of 20 N.

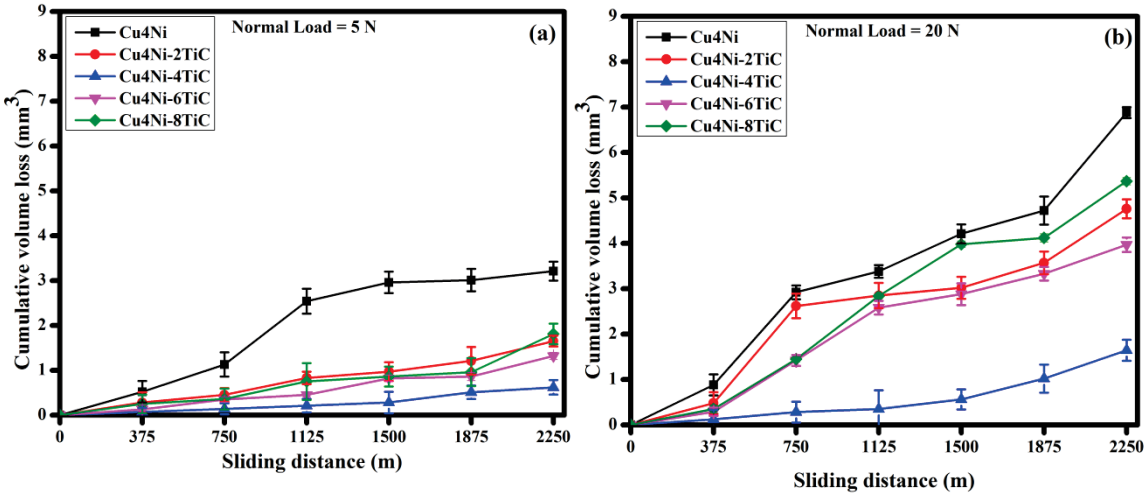

Fig.5.9: Variation of cumulative volume loss with sliding distance at normal load of (a) 5 N and (d) 20 N for a constant sliding speed of 1 m/s.

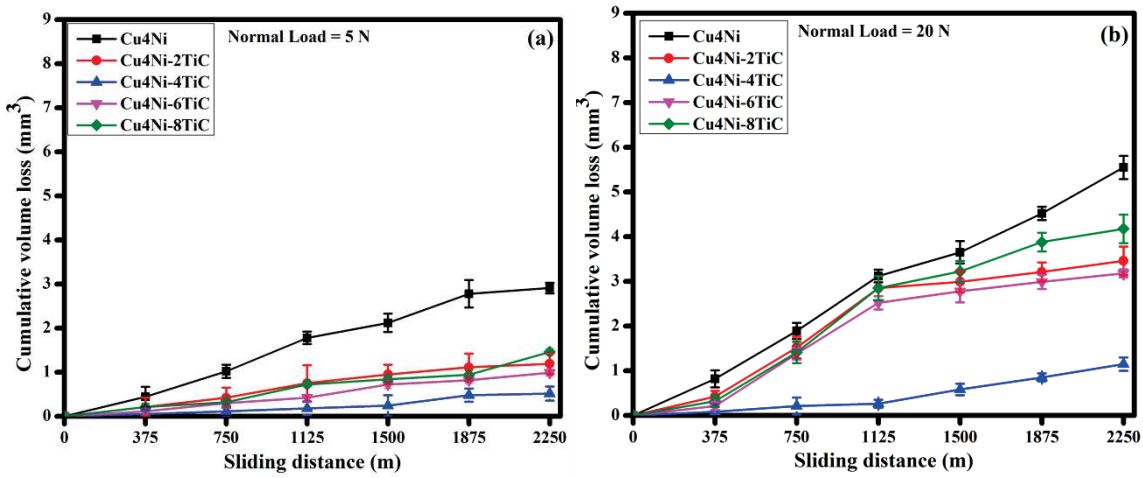

Fig.5.10: Variation of cumulative volume loss with sliding distance at normal load of (a) 5 N and (d) 20 N for a constant sliding speed of 0.75 m/s.

(ii) Variation of wear rate with normal load

The wear rate at a particular load has been estimated from the slope of the variation of cumulative volume loss with sliding distance presented in Fig.5.8 for Cu4Ni matrix alloy as well as for the various composites such as Cu4Ni-2TiC, Cu4Ni-4TiC, Cu4Ni-6TiC and Cu4Ni-8TiC by fitting the data points using linear least square fit and the variation of wear rate with normal load and at a constant speed of 1 m/s is shown in Fig.5.11. The wear rate increases almost linearly for all the materials used in the present study which could be seen from Fig. 5.11. However, the wear rate shown by Cu4Ni is the higher at all the normal loads. Among the composites, Cu4Ni-4TiC has shown the lowest rate of wear whereas the wear rates shown by other composites appear to fall in the same band at relatively lower loads but the difference in appears to increase with increasing load, especially, for Cu4Ni-8TiC, as can be observed in Fig. 5.11.

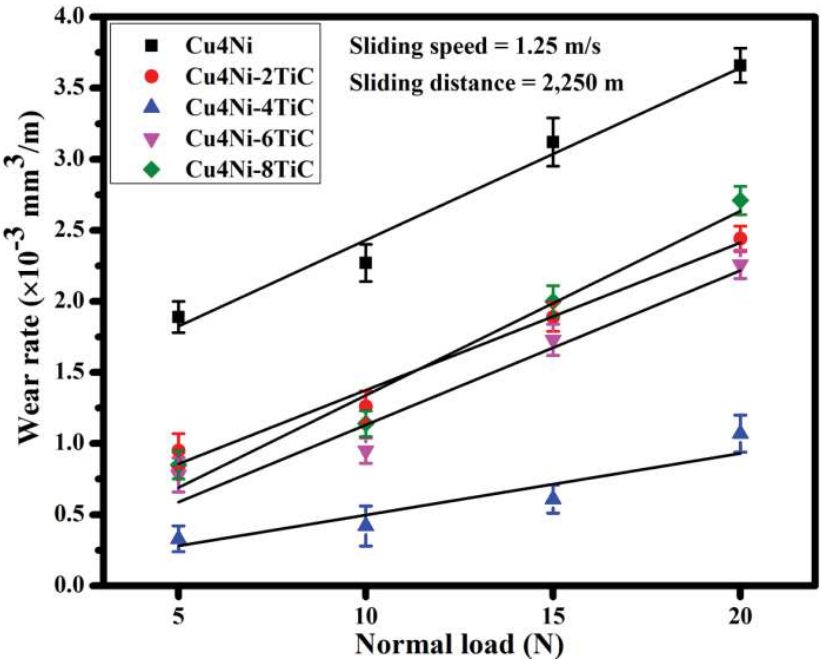

Fig.5.11: Variation of wear rate with normal load.

(iii) Variation of wear rate with sliding speed

Figures 5.12 (a) and (b) show the variation of wear rate of Cu4Ni, Cu4Ni-2TiC, Cu4Ni-4TiC, Cu4Ni-6TiC and Cu4Ni-8TiC with sliding speed at normal loads of 5 and

20 N. The wear rate has been observed to increase with increasing sliding speed for both the normal loads. The wear rate shown by Cu4Ni is the largest whereas that shown by Cu4Ni-4TiC is the smallest as evident from Figs 5.12 (a) and (b). The wear rate of Cu4Ni at 5 N load and sliding speed of 0.75, 1 and 1.25 m/s is 1.29, 1, 1.25 ($10^{-3}mm^3/m$), respectively, whereas the wear rate at 20 N load is 2.46, 3.06, 3.45($10^{-3}mm^3/m$), respectively. In case of Cu4Ni-4TiC composite the wear rate at load of 5 N is 0.22, 0.27, 0.34($10^{-3}mm^3/m$), respectively, and at 20 N load it is 0.51, 0.73, 1.06 ($10^{-3}mm^3/m$), respectively.

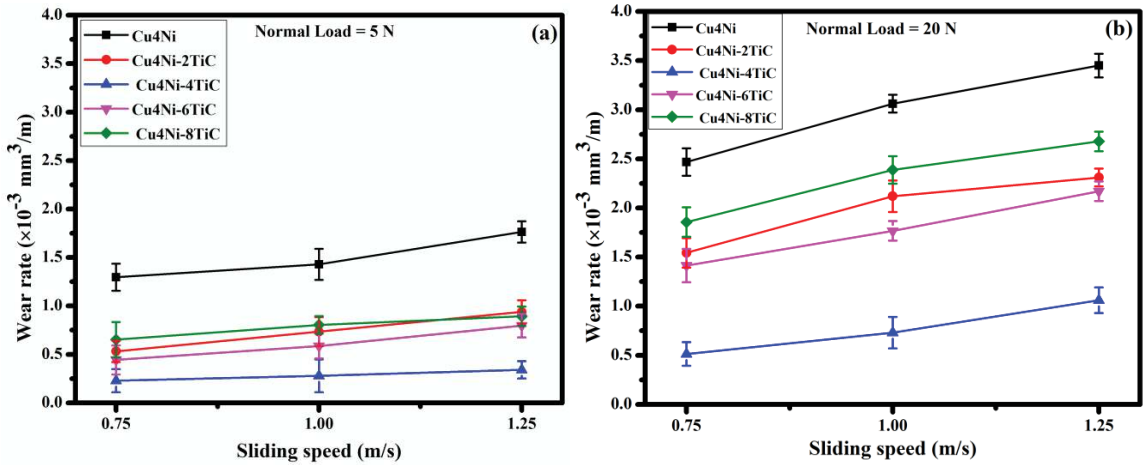

Fig.5.12: Variation of wear rate with sliding speed at normal load of (a) 5 N and (b) 20 N.

(iv) Variation of wear coefficient with TiC reinforcement

The wear coefficient has been estimated from the slope of the linear variation of wear rate with load, by multiplying it with the initial hardness of the corresponding material. Figure 5.13 shows the variation of wear coefficient with TiC reinforcement at constant sliding speed of 1.25 m/s. It can be observed from the Fig.5.13 that wear coefficient decreases up to Cu4Ni-4TiC containing 4 wt.% TiC beyond which it increases.

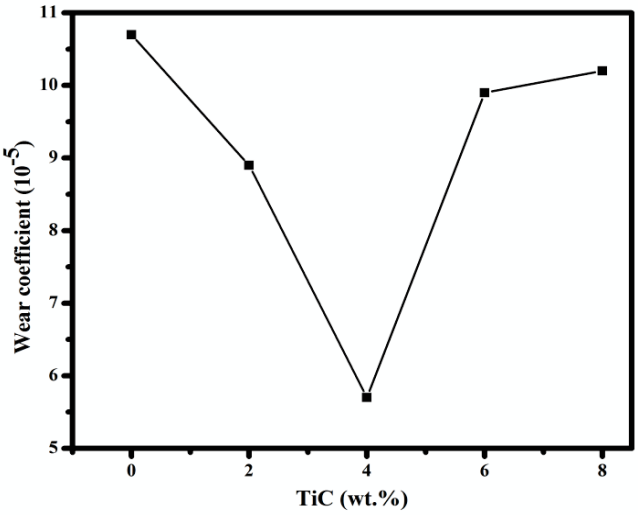

Fig. 5.13: Variation of wear coefficient with TiC reinforcement at constant sliding speed of 1.25 m/s.

.

(v) Variation of wear rate with amount of TiC

The effect of TiC content on the wear rate of Cu4Ni, Cu4Ni-2TiC, Cu4Ni-4TiC, Cu4Ni-6TiC and Cu4Ni-8TiC composites at normal loads of 5, 10, 15 and 20 N is shown in Fig. 5.14. It can be observed that the wear rate increases with increasing TiC content till 4 wt. % beyond which it increases, indicating that 4 wt.% TiC is the optimum addition under the conditions used in the present study.

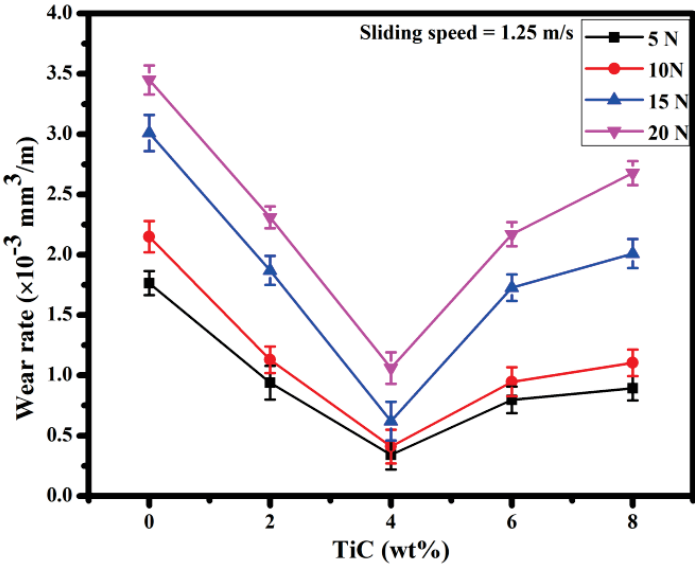

Fig.5.14: Variation of wear rate with TiC reinforcement at normal load of 5, 10, 15 and 20 N for a constant sliding speed of 1.25 m/s.

5.1.2 Examination of Sliding Surfaces

Figures 5.15 (a) to (c) show the SEM micrographs of the worn surfaces of Cu4Ni, Cu4Ni-4TiC and Cu4Ni-8TiC, respectively, after sliding through a distance of 2,250 at a normal load of 5 N and a constant sliding speed of 1.25 m/s. Some grooves running along the direction of sliding along with a transfer layer of wear debris could be observed on all the surfaces. However, the grooves appear to be deeper in case of Cu4Ni in comparison to those observed on the worn surface of Cu4Ni8TiC as evident from Figs. 5.15 (a) and (c). No grooves could be observed on the worn surface of Cu4Ni-4TiC which appears to be completely covered by the transfer layer as seen from Fig. 5.15 (b). The extent of transfer layer appears to be more the surface of Cu4Ni-8TiC in comparison to that of Cu4Ni. This may have a bearing on the observed friction and wear behavior of these materials.

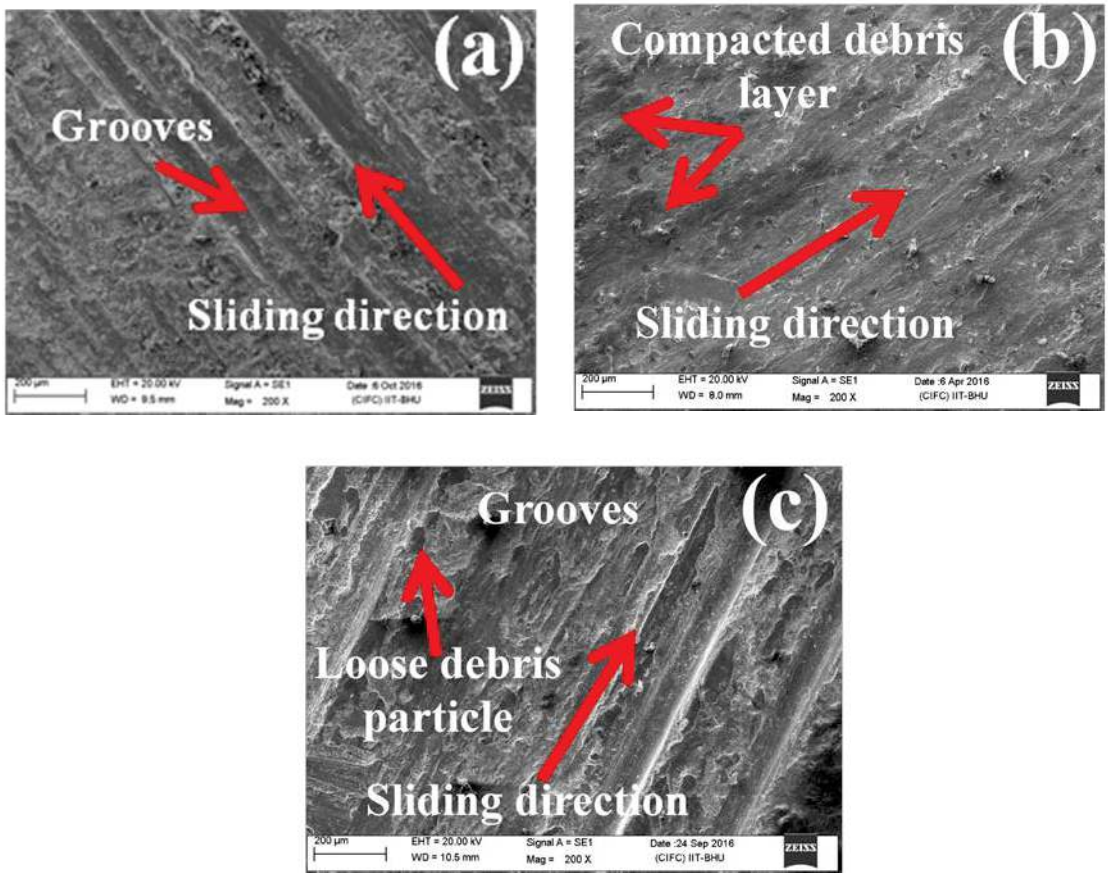

Fig.5.15: SEM micrographs of worn surface of (a) Cu4Ni matrix alloy, (b) Cu4Ni-4TiC and (c) Cu4Ni-8TiC composite at load of 5 N and sliding speed of 1.25 m/s.

SEM micrographs of the worn surfaces of Cu4Ni matrix alloy, Cu4Ni-4TiC and Cu4Ni-8TiC composites, respectively, at normal load of 10 N and a constant sliding speed of 1.25 m/s are shown in Figs 5.16 (a) to (c). A heavily torn surface could be seen in case of Cu4Ni with sign of delamination at some places as illustrated in Fig. 5.16 (a). However, the worn surfaces of CuNi-4TiC and CuNi-8TiC present some shallow grooves covered with the transfer layer as evident from Figs. 5.16 (b) and (c). Also, the extent of cover provided by transfer layer is more in case of Cu4Ni-4TiC in comparison to Cu4Ni-8TiC. Similar features have been observed on the worn surface of other composites, namely, Cu4Ni-2TiC and Cu4Ni-6TiC, hence, those have not been shown here.

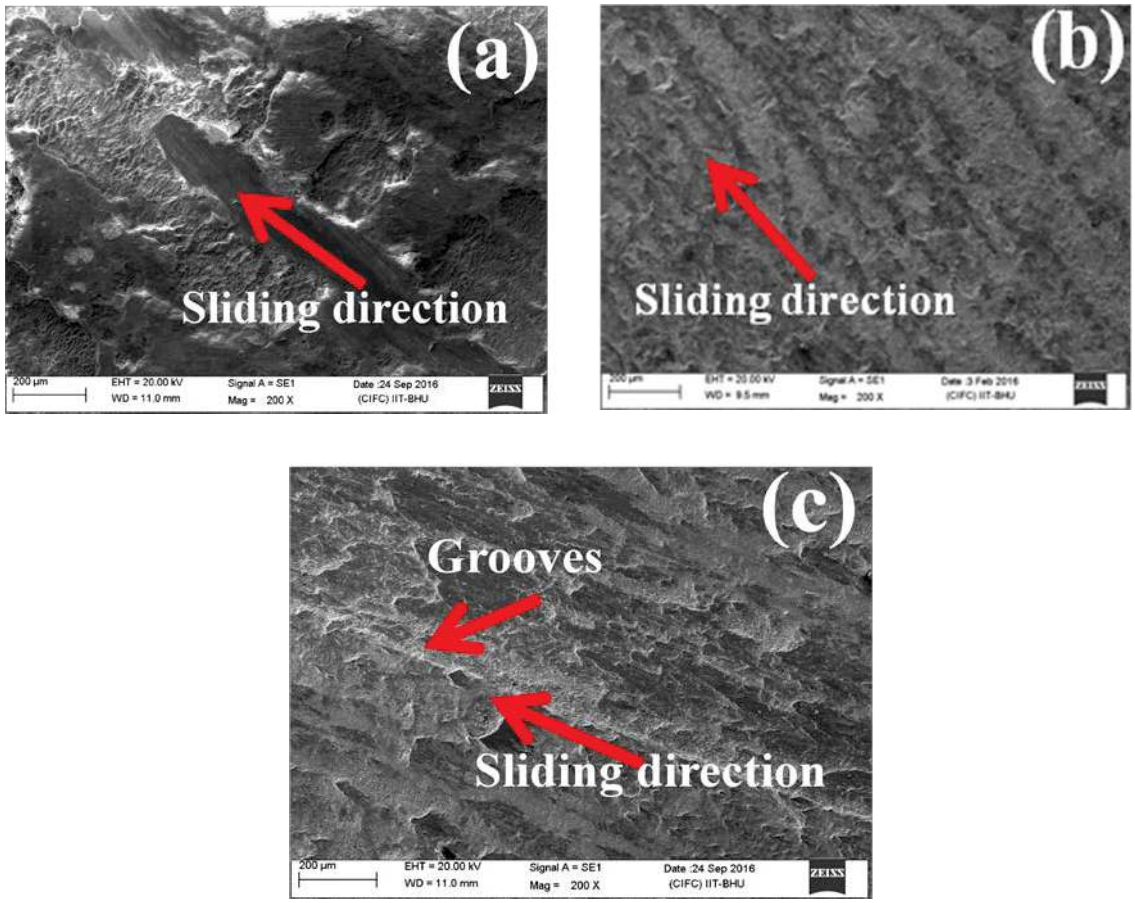

Fig.5.16: SEM micrographs of worn surface of (a) Cu4Ni matrix alloy, (b) Cu4Ni-4TiC and (c) Cu4Ni-8TiC composite at load of 10 N and sliding speed of 1.25 m/s.

Figures 5.17 (a) to (c) show the SEM micrographs of worn surfaces of Cu4Ni, Cu4Ni-4TiC and Cu4Ni-8TiC composites, respectively, at normal load of 15 N and a constant sliding speed of 1.25 m/s. The worn surface of Cu4Ni matrix alloy shows the presence of loosely bound transfer layer of wear debris from which some particles appear to have got detached as shown in Fig. 5.18 (a). However, the worn surfaces of the Cu4Ni-4TiC and Cu4Ni-8TiC present some grooves running parallel to the direction of sliding along with the presence of layer of debris as illustrated in Figs. 5.18 (b) and (c), respectively. The transfer layer appears to have got delaminated in case of Cu4Ni-8TiC as indicted by the arrow marked on the micrograph shown in Fig. 5.18 (c).

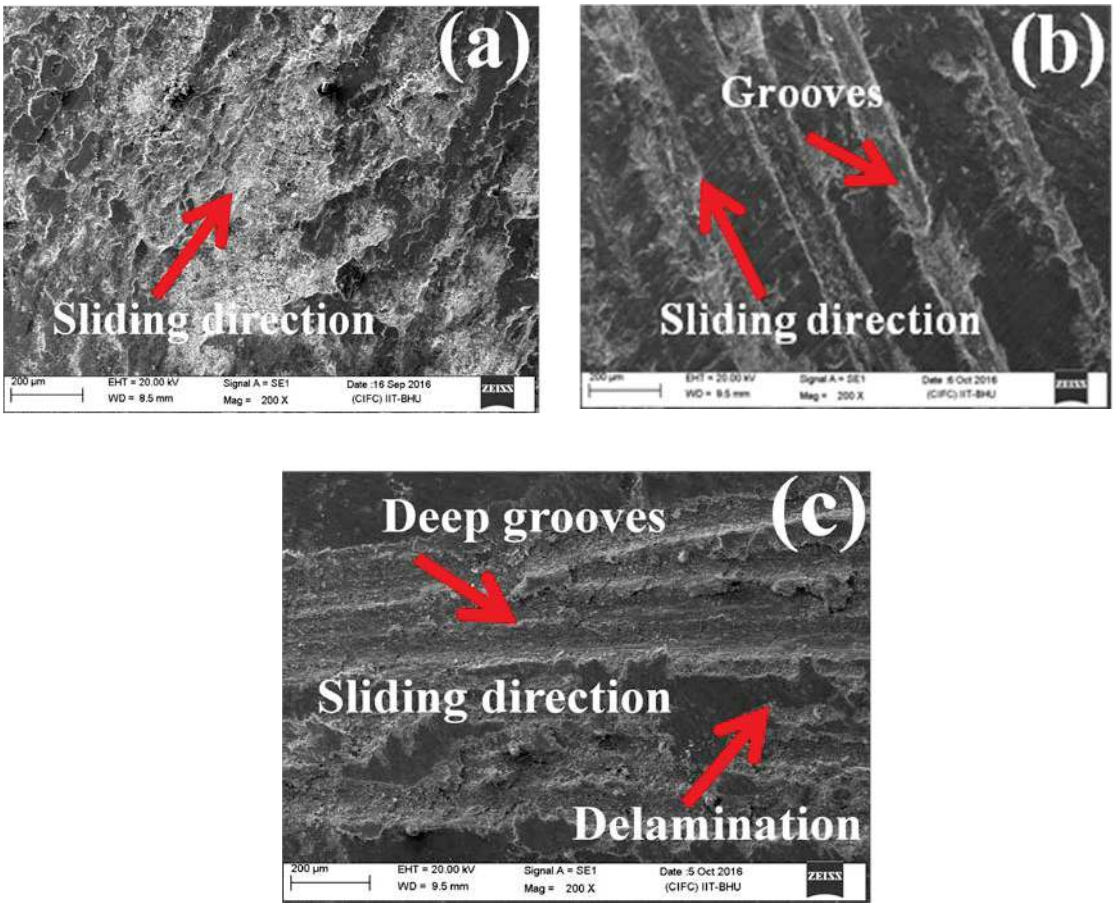

Fig.5.17: SEM micrographs of worn surface of (a) Cu4Ni matrix alloy, (b) Cu4Ni-4TiC and (c) Cu4Ni-8TiC composite at load of 15 N and sliding speed of 1.25 m/s.

SEM micrographs of the worn surface of Cu4Ni, Cu4Ni-4TiC and Cu4Ni-8TiC slid under a normal load of 20 N at a constant sliding speed of 1.25 m/s are shown in Figs.5.18 (a) to (c), respectively. Figure 5.18 (a) shows some sign of plastic deformation and the detachment of particles from the loosely bound transfer layer at several places. The transfer layer appears to be smooth and well compacted on the surface of Cu4Ni-4TiC as seen from Fig. 5.18 (b). The worn surface of Cu4Ni-8TiC shown in Figure 5.18 (c) also reveals the presence of a transfer layer but it appears to be loosely bound. One can also observe the delamination or detachment of this layer of wear debris at several places.

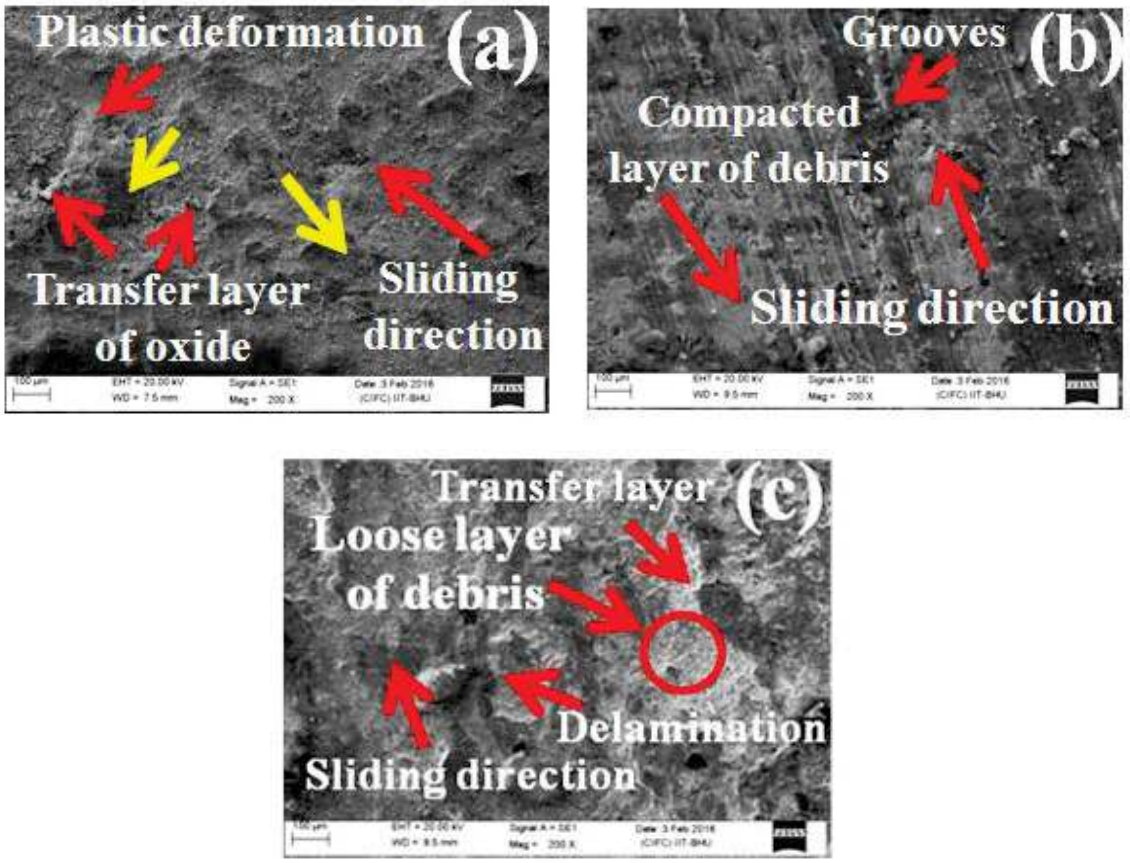

Fig.5.18: SEM micrographs of worn surface of (a) Cu4Ni matrix alloy, (b) Cu4Ni-4TiC and (c) Cu4Ni-8TiC composite at load of 20 N and sliding speed of 1.25 m/s.

EDS analysis was conducted on the worn tracks of the materials to reveal the presence of elements at the worn surface. Figures 5.19 (a) to (e) show the EDS spectrum

of worn surfaces of Cu4Ni, Cu4Ni-2TiC, Cu4Ni-4TiC, Cu4Ni-6TiC, and Cu4Ni-8TiC, respectively, at a normal load of 20 N and a constant sliding speed of 1.25 m/s.

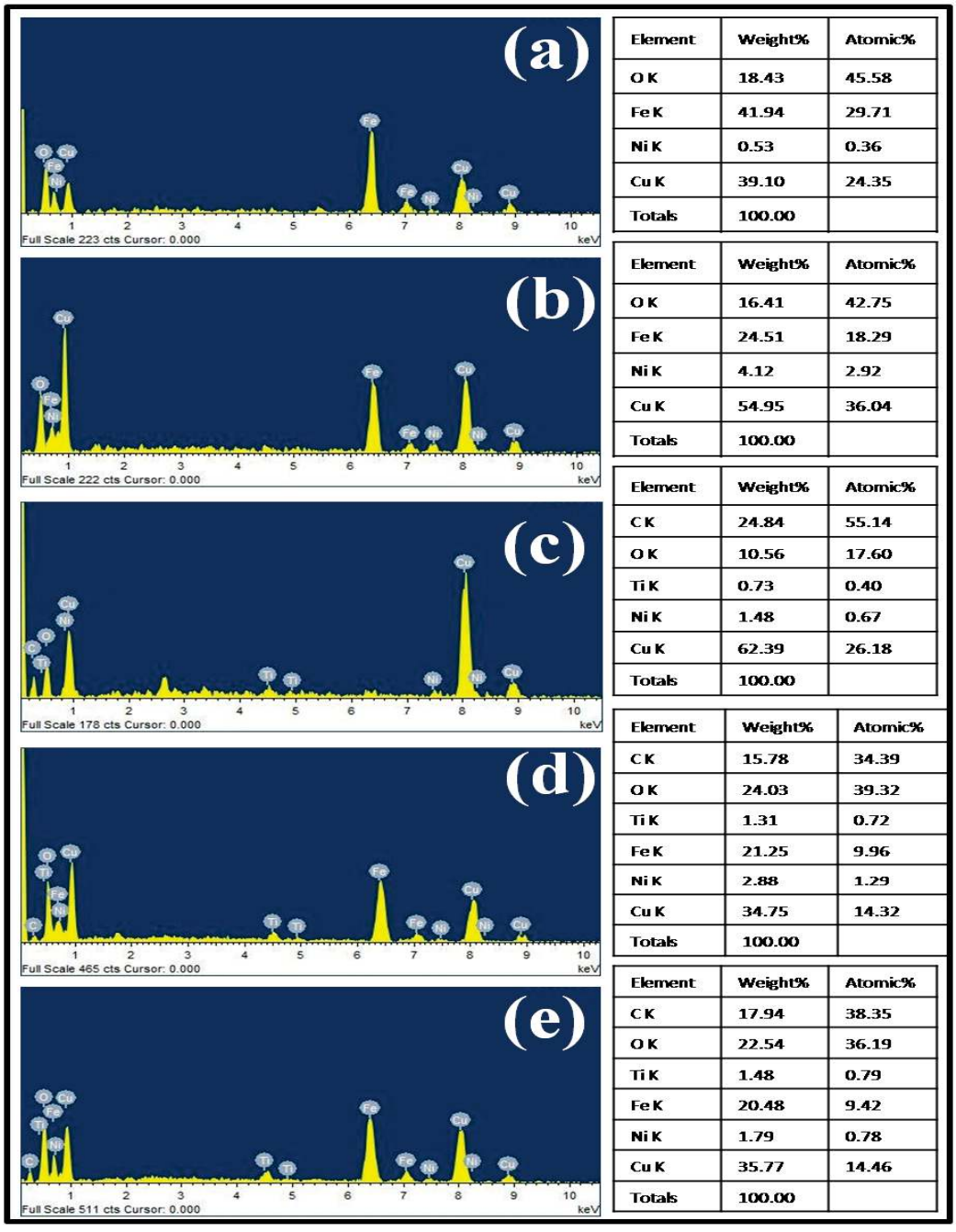

Element	Weight%	Atomic%
O K	18.43	45.58
Fe K	41.94	29.71
Ni K	0.53	0.36
Cu K	39.10	24.35
Totals	100.00	

Element	Weight%	Atomic%
O K	16.41	42.75
Fe K	24.51	18.29
Ni K	4.12	2.92
Cu K	54.95	36.04
Totals	100.00	

Element	Weight%	Atomic%
C K	24.84	55.14
O K	10.56	17.60
Ti K	0.73	0.40
Ni K	1.48	0.67
Cu K	62.39	26.18
Totals	100.00	

Element	Weight%	Atomic%
C K	15.78	34.39
O K	24.03	39.32
Ti K	1.31	0.72
Fe K	21.25	9.96
Ni K	2.88	1.29
Cu K	34.75	14.32
Totals	100.00	

Element	Weight%	Atomic%
C K	17.94	38.35
O K	22.54	36.19
Ti K	1.48	0.79
Fe K	20.48	9.42
Ni K	1.79	0.78
Cu K	35.77	14.46
Totals	100.00	

Fig.5.19: EDS of worn surface of (a) Cu4Ni matrix alloy, (b) Cu4Ni-2TiC (c) Cu4Ni-4TiC, (d) Cu4Ni-6TiC, and (d) Cu4Ni-8TiC composite at load of 20 N and sliding speed of 1.25m/s.

The spectrum corresponding to Cu4Ni given in Fig. 5.19 (a) shows the presence of O, Fe, Ni and Cu at the worn surface, Fe would have come from through transfer of material from counterface. The EDS spectrum corresponding to composites show the presence of Ti and C in addition to Cu, Ni, Fe and O as evident from Figs. 5.19 (b) to (e).

SEM micrographs of the sliding surface of Cu4Ni, Cu4Ni-4TiC, Cu4Ni-8TiC worn at a normal load of 5 N and sliding speed of 0.75 m/s are depicted in Figs. 5.20 (a) to (c) which show the presence of a transfer layer of wear debris on all the surfaces but with a different extent of coverage of the sliding surface. Fig. 5.20 (a) corresponding to Cu4Ni shows the presence of a transfer layer of wear debris covering about 50 % of area of the worn surface. However, the detachment of transfer layer at few places in the covered region could also be seen from the micrograph.

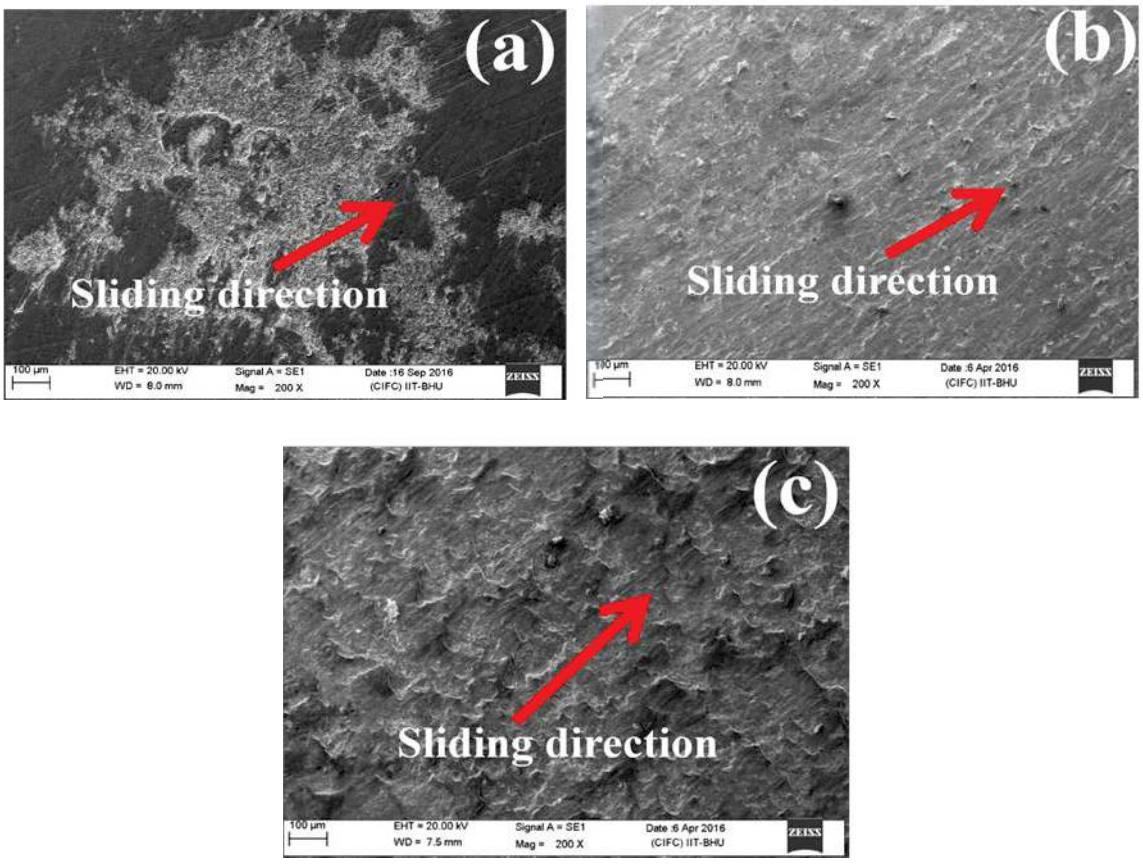

Fig.5.20: SEM micrograph of worn surface of (a) Cu4Ni, (b) Cu4Ni-4TiC and (c) Cu4Ni-8TiC composite at sliding speed of 0.75 m/s and at load of 5 N.

The worn surfaces of Cu4Ni-4TiC and Cu4Ni-8TiC shown, respectively, in Figs. 5.20 (b) and 5.20 (c) are seen to be totally covered by the transfer layer. However, the transfer layer appears to have got detached at a few places in case of Cu4Ni-8TiC as shown by arrows. Figure 5.21 reveals the SEM micrographs of worn surface of (a) Cu4Ni, (b) Cu4Ni-4TiC and (c) Cu4Ni-8TiC composite at a sliding speed of 0.75 m/s and at a load of 20 N. Deeper grooves can be observed on the surface of Cu4Ni whereas shallow grooves covered with the transfer layer seen in case of Cu4Ni-4TiC and Cu4Ni-8TiC.

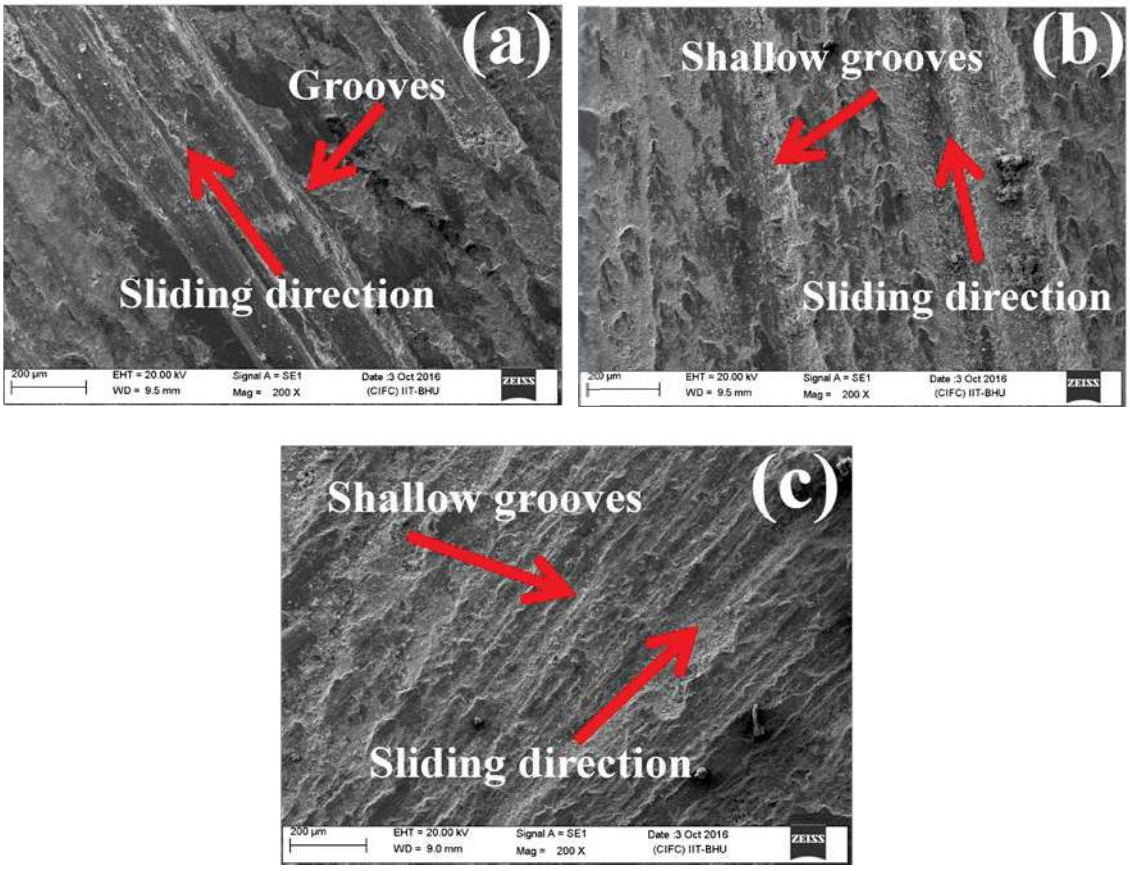

Fig.5.21: SEM micrograph of worn surface of (a) Cu4Ni, (b) Cu4Ni-4TiC (c) Cu4Ni-8TiC composite at sliding speed of 0.75 m/s and at load of 20 N.

Figures 5.22 (a) to (c) show the SEM micrographs of worn surfaces of Cu4Ni, Cu4Ni-4TiC and Cu4Ni-8TiC at a sliding speed of 1 m/s and a load of 5 N whereas the same for 20 N load are presented in Fig. 5.23. Some deeper grooves running parallel to sliding direction and covered at places by transfer layer of wear debris could be observed on the surface Cu4Ni and Cu4Ni-8TiC as evident from Figs. 5.22 (a) and (c) However, the worn surface of CuNi-4TiC reveals the presence of shallow grooves which appear to be covered by the transfer layer of debris as observed in Fig. 5.22 (b). Similar features could be observed on the surfaces for 20 N load as evident from Figs. 5.23 (a) to (c). However, the groves appear to be relatively deeper for the surface worn at the highest load of 20 N in comparison to those slid at the lowest load of 5 N which could be judged by comparing Figs. 5.22 and 5.23.

Figure 5.24 (a, b) depicts the SEM micrographs of wear debris of Cu4Ni matrix alloy and Cu4Ni-4TiC composite at a constant sliding speed of 1.25 m/s under the load of 20 N. It can be observed that wear debris of Cu4Ni matrix alloy is comparatively bigger in size because adhesive wear is taking place. In case of Cu4Ni-4TiC composite, the wear debris is comparatively small and equiaxed.

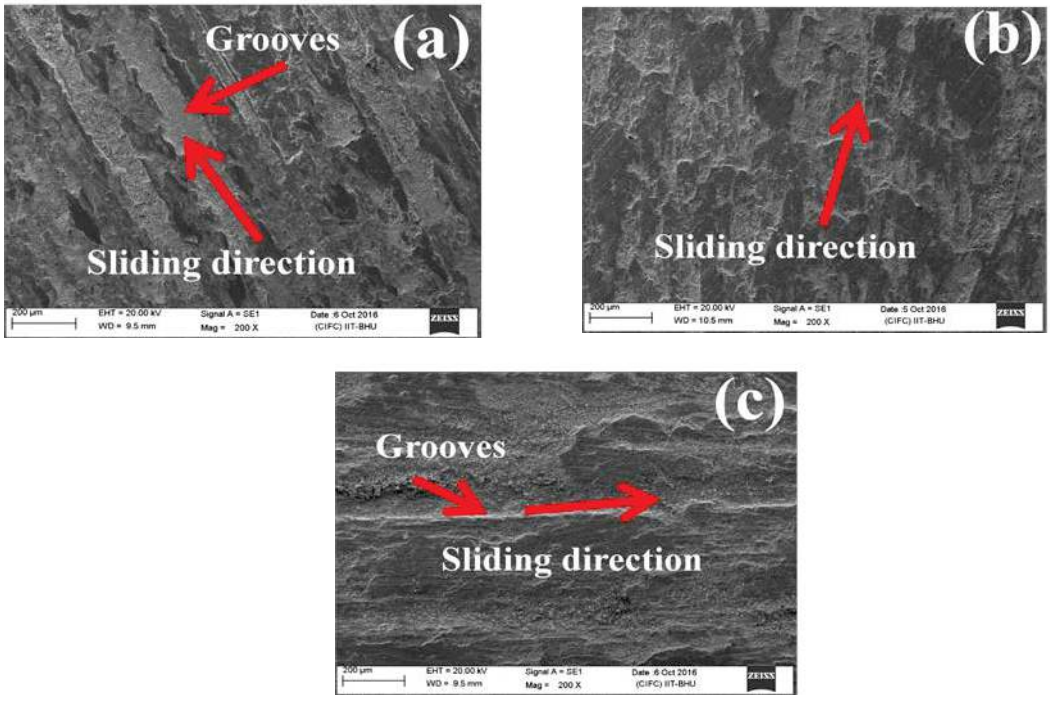

Fig.5.22: SEM micrograph of worn surface of (a) Cu4Ni, (b) Cu4Ni-4TiC and (c) Cu4Ni-8TiC composite at sliding speed of 1 m/s and at load of 5 N.

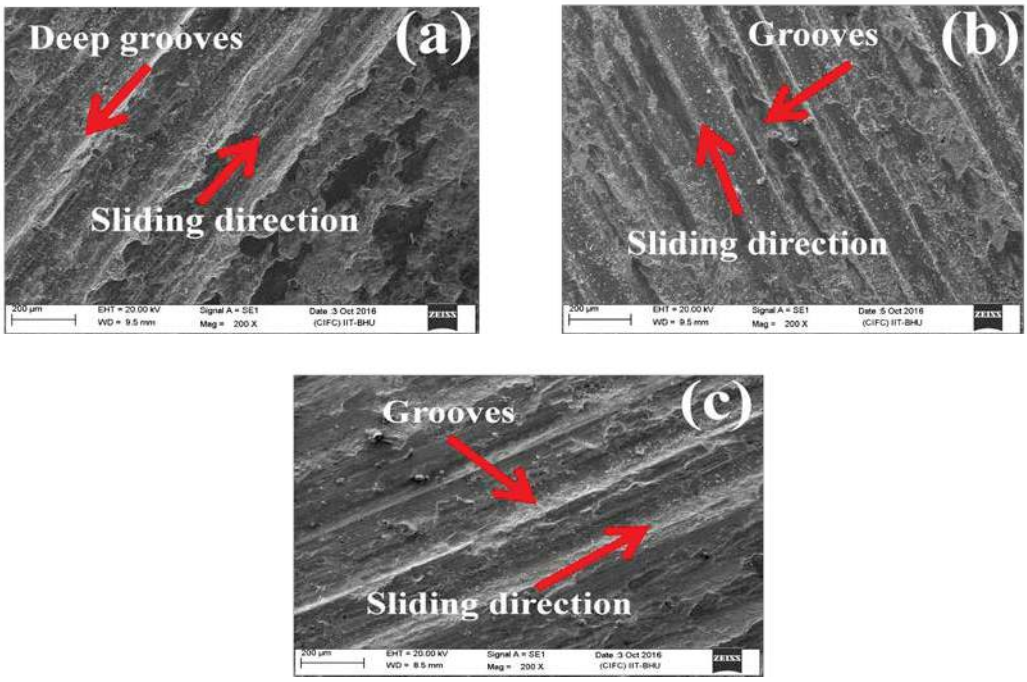

Fig.5.23: SEM micrograph of worn surface of (a) Cu4Ni, (b) Cu4Ni-4TiC and (c) Cu4Ni-8TiC composite at sliding speed of 1 m/s and at load of 20 N.

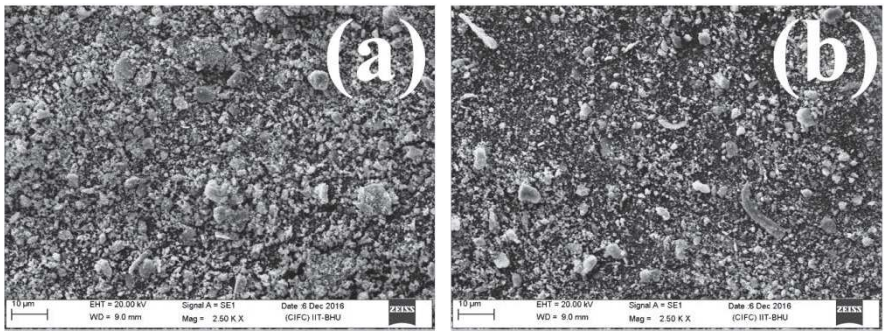

Fig.5.24: SEM micrographs of wear debris of (a) Cu4Ni matrix alloy and (b) Cu4Ni-4TiC.

5.2 DISCUSSION

The typical variation of average coefficient of friction with sliding distance at normal load of 5 N, 10 N, 15 N and 20 N for Cu4Ni, Cu4Ni-2TiC, Cu4Ni-4TiC, Cu4Ni-6TiC and Cu4Ni-8TiC composites at a constant sliding speed of 1.25 m/s against the EN31 steel counter face are shown in Figs.5.1 (a) to (d). It is observed from Figs. 5.1 (a) to (d) that nature of coefficient of friction is very much fluctuating with respect to sliding distance and no certain trend is observed. Similarly, the coefficient of friction is fluctuating with sliding distance as shown in Figs 5.2 and 5.3 at sliding speeds of 1 m/s

and 0.75 m/s and normal loads of 5 N and 20 N, respectively. The cause for the fluctuation can be attributed to the disparity in contact that occurs when the sample and the counterface are evolving to develop a better surface conformity.

The variations of average coefficient of friction with normal load and TiC content at a constant sliding speed of 1.25 m/s after sliding through a distance of 2,250 m for Cu4Ni, Cu4Ni-2TiC, Cu4Ni-4TiC, Cu4Ni-6TiC and Cu4Ni-8TiC composites are shown respectively, in Figs. 5.4 and 5.7. One could observe that the friction coefficient increases with increasing both the normal load and the amount of TiC. The friction coefficient increases with the increasing TiC content in the composites at a particular load as evident from Fig. 5.7, which may be attributed to the abrasion caused by the TiC particles that are detached from the matrix and get trapped between the contacting surfaces. At relatively higher loads, more particles are expected to get detached with increasing load which may promote three body abrasion resulting in an increased friction coefficient in the composites if the particles are not able to form a well compacted layer on the surface. An increase in the TiC content further aggravates the situation as more number of particles now gets detached, thereby aiding abrasion. Hence, the friction coefficient increased with both the load and the TiC content. A relatively lower friction coefficient shown by Cu4Ni may be attributed to the relatively soft nature of the matrix in comparison to the composites as well as the absence of any abrasive action. Apart from this, the behavior of the transfer layer formed on the surface and its extent also plays an important role in governing the friction and wear phenomenon. It can be observed from the SEM micrographs shown in Fig.5.15 (a) corresponding to the lowest load of 5 N used in the present study that no loose particles are appearing in case of Cu4Ni matrix alloy and thus there is absence of three body abrasion. Also, at the lowest load of 5 N, there appears to be a little formation of transfer layer on the surface of Cu4Ni as seen from Fig. 5.15 (a) which might have resulted in metal-metal contact giving rise to friction. A well compacted transfer layer of debris can be observed on the surface in case of Cu4Ni-4TiC composite as shown in Fig. 5.15 (b). The layer inhibits metal-metal contact and provides low shearing strength junction at the interface which results in a reduced friction coefficient. The presence of transfer layer could also be observed on the surface of

Cu4Ni-8TiC composite as shown in Fig. 5.15 (c), but the particles appear to be loosely bound. The loose particles enhance the probability of three body abrasion and hence the friction coefficient shown by the composite containing the largest wt.% of TiC is the highest in the present study. At maximum load of 20 N, it can be observed from the SEM micrographs shown in Fig.5.18 (a) corresponding to Cu4Ni that this layer appears to have been detached at some places (marked by yellow arrow on the micrograph) allowing thus the metal-metal contact to take place. Also, the extent of cover provided by this layer appears to be relatively less in comparison to the one formed on the surface of the composites Cu4Ni-4TiC and Cu4Ni-8TiC which could be seen from a comparison of Figs. 5. 18 (a), (b) and (c).The worn surface of Cu4Ni-4TiC appear to be mostly covered by the well compacted transfer layer as seen from Fig. 5.18 (b) whereas the transfer layer appears have got delaminated at some places from the surface of Cu4Ni-8TiC as shown in Fig. 5.18 (c). This might have allowed metal-metal contact and a consequent increase in friction coefficient. SEM micrographs presented in Fig. 5.16 and 5.17 at the loads of 10 and 15 N may also be explained on the similar basis.

The variations of average coefficient of friction of Cu4Ni, Cu4Ni-2TiC, Cu4Ni-4TiC, Cu4Ni-6TiC and Cu4Ni-8TiC composites with sliding speed (0.75, 1 and 1.25 m/s) at the lowest and the highest normal loads of 5 N and 20 N are shown in Fig.5.5 (a) and (b). It is observed that average coefficient of friction increases with increase in sliding speed for all the materials used in the present investigation. The reason for the increase in the coefficient of friction of Cu4Ni alloy with increase in sliding speed may be attributed to the fact that when sliding contact takes place between the contacting surfaces then there is chances that surface of the matrix alloy in contact with the counterface can easily gets oxidized in the air up to a particular level and tends to form a thin transfer layer on the surface. This transfer layer is responsible to separate the two metallic surfaces and also acts as a low shear strength film resulting in low friction. However, the contact pressure is high enough to rupture the thin transfer layer in present sliding conditions. When the transfer layer ruptures, a clean metal-metal contact and high adhesion occurs. As a result, the transfer layer cannot continuously prevent the direct metal-metal contact. In addition, during the sliding an existing stress at the interface results in plastic

deformation of copper matrix. Due to this repetitive thin transfer layer formation and direct metal-metal contact at the lower sliding speed, low friction is observed. As the speed increases, the chances of formation of a thicker and more brittle transfer layer increase due to high interface temperature and continuous oxidation. The transfer layer on the Cu4Ni is observed to contain Fe which might have been transferred from the counterface as evident from the EDS spectra shown in Fig. 5.19 (a). This results in an increase in the shear strength of the transfer layer. Hence, a larger shear force is needed to shear the junctions which leads to an increase in the friction coefficient with increasing speed of sliding. Similar observations of increase in the coefficient of friction of copper alloy with increase in sliding speed have been reported by Celikyurek et al. (2011). However, the increase in friction coefficient with speed for composites may be attributed to the presence of transfer layer of debris containing TiC particles which provide abrasive action depending up on the fact that whether they are loose or tightly bound in the layer as explained earlier. A comparison of Figs. 5.20 (b, c), 5.22 (b, c) and 5.15 (b, c), which show the worn surfaces at the lowest normal load 5 N and sliding speeds of 0.75, 1.0 and 1.25 m/, clearly indicate that the extent of cover provided by the transfer layer is more in case of Cu4Ni-4TiC in comparison to that on Cu4Ni-8TiC. Also, the extent of cover is observed to decrease with increasing speed of sliding despite the chances of a better compaction with increasing frictional heat at relatively higher speed of sliding. The layer appears to have got detached at few places in Cu4Ni-8TiC. Similar features could also be observed on the sliding surfaces shown in Figs. 5.21 (b, c) and 5.23 (b, c) corresponding to the highest load of 20 N used in the present study. Also, at relatively higher speeds there are more chances of TiC pull out due to increased frictional heat during sliding. The situation further worsens in the composites containing relatively larger amount of TiC as more and more particles are expected to get detached from the matrix which may give rise to increased friction. This may explain the increase in friction coefficient with increasing speed in the composites containing increasing amounts of TiC as shown in Fig. 5.5. Among the composites, Cu4Ni-4TiC has shown the lowest coefficient of friction at all the loads and speeds and this may be attributed to the highest hardness shown by this composite in the present study. A substrate with a higher hardness has been shown to support a relatively thicker layer of the oxide or wear debris which is able to inhibit

metal-metal contact more effectively (Saka et al., 1977). This may explain the observed frictional behavior in composites and it is also evident from Fig. 5.6 which shows the variation of friction coefficient with hardness of materials used in the present investigation.

Figures 5.8 (a) to (d) show the variation of cumulative volume loss with sliding distance for all the materials investigated in the present study under different loads of 5, 10, 15, 20 N and at a constant sliding speed of 1.25 m/s. The cumulative volume loss increases almost linearly with increasing sliding distance which was confirmed through curve fitting by linear least square fit. It can be observed that the volume loss of the matrix alloy is consistently higher at all the normal loads in comparison to the composites, which is not surprising because the hard TiC particles provide a shield to the relatively softer matrix during sliding and enhance the load bearing capacity of the composites leading to a lower loss of material (Kumar et al., 2014; Nemati et al., 2011).The role of the reinforcement particles is to support the contact stresses preventing high plastic deformations and abrasion between contacting surfaces and hence to reduce the amount of worn material as suggested by Hassan et al., (2009) also. Among the composites, the one containing 4 wt.% TiC i.e., Cu4Ni-4TiC has shown the lowest volume loss consistently at all the normal loads, followed by Cu4Ni-6TiC, Cu4Ni-8TiC and Cu4Ni-2TiC in increasing order. This may be explained on the basis of the hardness of the composites. Since, the hardness of Cu4Ni-4TiC is the highest in the present study, it has shown the smallest cumulative volume loss and that of Cu4Ni -2TiC is the lowest among the composites, hence it has the largest volume loss. The other factor may be the nature of transfer layer and the extent of cover provided by it to the underlying material which helps in reducing the metal-metal contact as explained earlier. However, the cumulative volume loss has also been observed to increase with increasing load for a particular material. This may be attributed to the fact that more number of asperities come into contact with increasing load and as a result the amount of worn material increases as indicated by Hassan et al. (2008) who have also reported similar observations. Similar, behavior has been observed at other speeds of 1.0 m/s and 0.75 m/s as evident from Figs. 5.9 (a, b), and 5.10 (a, b) which show the variation of cumulative

volume loss with sliding distance at normal loads of 5 N and 20 N for a constant sliding speed of 1 m/s and 0.75 m/s, respectively.

The wear rate at a particular load has been calculated from the slope of the variation of cumulative volume loss with sliding distance for Cu4Ni matrix alloy as well as for the composites such as Cu4Ni-2TiC, Cu4Ni-4TiC, Cu4Ni-6TiC and Cu4Ni-8TiC by fitting the data points through linear least square fit and the variation of wear rate with normal load is shown in Fig.5.11. It can be seen from Fig. 5.11 that the wear rate increases almost linearly with the load following Archard's law which states that wear rate is directly proportional to the normal load but inversely proportional to the hardness of the softer of the two mating materials (Archard, 1953). It can be expressed mathematically as,

$$w = k\frac{LS}{H} \tag{5.1}$$

where W is wear volume loss, K is the wear coefficient, L is the applied load, S is the sliding distance and H is the hardness of softer material. However, the composites have a lower wear rate than the Cu4Ni at all the loads, which may be attributed to the higher hardness of the composites in comparison to the Cu4Ni matrix alloy. The increasing rate of wear with normal load may be explained on the basis of the generation of more debris at relatively higher load leading to a higher loss of material and thus, the wear rate. In case of matrix alloy, it can be presumed that there is a possibility of direct metal-metal contact and this phenomenon may promote the adhesive wear mechanism and consequently the plastic deformation takes place and the wear rate of matrix alloy increases as compared to the composite specimens. A comparison of Figs. 5.15 (a), 5.16 (a), 5.17 (a) and 5.18 (a) which correspond to the worn surface of Cu4Ni at loads of 5, 10, 15 and 20 N, respectively, shows that Cu4Ni has deeper grooves along with signs of plastic deformation and presence of transfer layer with increasing loads. However, the extent of cover provided by the transfer layer is relatively lesser in comparison of those of the composites as seen from Figs. 5.15 to 5.18, which might have given rise to more wear rate in Cu4Ni in comparison to composites as explained earlier. Among the composites, Cu4Ni-4TiC has shown the lowest rate of wear in comparison to other composites. This may be attributed to the relatively higher hardness of this composite in

comparison to other composites due to which it is able to support a relatively thicker transfer layer. The other reason may the extent of cover provided by the transfer layer which is helpful in protecting the underlying material against wear. One could see that the extent of cover provided by the transfer layer is more in case of CuNi-4TiC in comparison to Cu4Ni-8TiC at all the normal loads as evident from a comparison of Figs. 5.15 (b, c) to 5.18 (b, c) which shows that the debris is either loose in case of Cu4Ni-8TiC or it has delaminated from several places due to the lower holding capability of Cu4Ni-8TiC caused by its relatively lower hardness. The wear mechanism in the Cu4Ni alloy appears to be a mix of oxidative wear which can be judged from the presence of oxygen in the EDS spectra shown in Fig. 5.19 (a) and plastic deformation which is evident from the SEM micrographs shown in Figs. 5.15 (a) to 5.18 (a). The wear mechanism in the composites appears to be a mix of oxidative wear which is evident from the presence of oxygen EDS spectra shown in Fig. 5.19 (b to e) and abrasive due to the presence of hard TiC particles as evident from Figs. 5.15 to 5.18 which show the presence of abrasive grooves running parallel to sliding direction. However, at some places these grooves appeared to be covered by the transfer layer of the debris.

The variation of wear rate of Cu4Ni, Cu4Ni-2TiC, Cu4Ni-4TiC, Cu4Ni-6TiC and Cu4Ni-8TiC composites with sliding speed (0.75, 1 and 1.25 m/s) at normal loads of 5 N and 20 N is shown in Fig.5.12 (a) and (b), respectively. It is observed that wear rate increases with increase in sliding speed. Also, the wear rate shown by the Cu4Ni alloy is the largest and that shown by Cu4Ni-4TiC is the smallest. The increase in wear rate with increasing speed at a particular load may be attributed to the increased frictional heating which results in softening of the surface increasing thereby the possibility of the deeper digging by the hard asperities of the counterface. This digging results in more loss of material and consequently the increased wear rate. The extent of softening may be more in Cu4Ni in comparison to the composites because of the presence of hard TiC particles. Hence, the wear rate shown by the Cu4Ni is more in comparison to composites at each speed for a particular load as evident from Fig. 5.12. Another factor contributing to the increased rate of wear with increasing speed in Cu4Ni alloy could be the nature of transfer layer, its extent and the delamination under a particular condition of load and

speed. One could see that at a load of 5 N, the transfer layer is more compact at the lowest speed of 0.75 m/s and no deeper grooves are visible (Fig. 5.20 (a)) whereas the layer appears to be torn at several places with the presence of deeper grooves in case of 1.0 and 1.25 m/s as evident from Figs. 5.22 (a) and 5.15 (a) which give rise to more wear rate with increasing speed. The behavior at the highest load of 20 N shown in Fig. 5.12 (b) may also be explained on similar lines as evidenced by Figs. 5.21 (a), 5.23 (a) and 5.18 (a). As far as composites are concerned; the softening may result in the particle pull out from the matrix and consequent generation of wear debris. The debris particles promote the three body abrasion if they do not get compacted to form a transfer layer. One could observe that the transfer layer has covered the entire area of the micrograph given in Fig. 5.20 (b) corresponding to Cu4Ni-4TiC at the lowest load of 5 N and a speed of 0.75 m/s whereas the transfer layer appears to have fractured at relatively higher speeds of 1.0 and 1.25 m/s giving rise to larger wear rate as evident form Figs. 5.22 (b) and 5.15 (b). Similar observations can be found for the 20 N load in case of Cu4Ni-4TiC which are evident from Figs. 5.20 (b), 5.23 (b) and 5.18 (b). The wear behavior of Cu4Ni-8TiC with increasing speed may also be explained on the similar lines for the load of 5 N as seen from Figs.5.20 (c), 5.22 (c), 5.15 (c) and Figs. 5.21 (c), 5.23 (c) and 5.18 (c) for the load of 20 N. However, the lowest wear rate shown by Cu4Ni-4TiC may again be attributed to its relatively higher hardness and ability to hold a relatively thicker transfer layer of debris as explained earlier.

The wear coefficient has been estimated from the slope of the linear variation of wear rate with load, *V/SL*, taken from Fig. 5.11 by multiplying it with the initial hardness of the corresponding material. The wear coefficient may be interpreted as wear rate per unit real area of contact. Figure 5.13 shows the variation of wear coefficient with TiC reinforcement. The wear coefficient decreases upto Cu4Ni-4TiC composite and after that it increases for Cu4Ni-6TiC and Cu4Ni-8TiC composites. The decrease in wear coefficient till 4 wt.% TiC may be attributed to the decreasing wear rate dominating over the decrease in real area of contact due to increasing hardness. However, beyond 4 wt.% the increasing wear rate dominates over increasing real area of contact due to decreased hardness resulting thus in a higher wear coefficient as evident from Fig. 5.13.

The variation of wear rate with amount of TiC for Cu4Ni, Cu4Ni-2TiC, Cu4Ni-4TiC, Cu4Ni-6TiC and Cu4Ni-8TiC composites at normal loads of 5, 10, 15 and 20 N is shown in Fig.5.14. It can be observed from Fig. 5.14 that the wear rate decreases up to the addition of 4 wt.% of TiC beyond which it increases till 8 wt.% TiC. The observed behavior may be attributed to the relatively higher hardness, the extent of the cover provided by the transfer layer and ability to hold a thicker transfer layer as explained earlier.

The wear debris of Cu4Ni matrix alloy as shown in Fig.5.24 (a) is comparatively bigger in size because adhesive wear is taking place and thus plastic deformation occurs. The generation of fine wear debris of Cu4Ni-4TiC as depicted in Fig.5.24 (b) is attributed to an abrasive micro-cutting effect (Li et al. 2015). The other cause for the smaller wear debris is due to the higher hardness of composites (Larionova et al. 2014).

The study of friction and wear presented above indicates that the amount of second phase and its distribution plays a crucial role in dictating the tribological behavior of composite materials. The increasing amount of TiC till 4 wt.% in Cu4Ni matrix imparts hardness to these composites, which in turn, results in lowering of real area of contact during dry sliding. The lower is the real area of contact, the lower will be the wear rate. Hence, the wear rate is observed to decrease linearly with increasing amount of TiC till addition of 4 wt.%, beyond which it increases due to the relatively lower hardness of composites (containing 6 and 8 wt. % TiC) caused by the agglomeration of TiC particles. The observed variation of friction coefficient as well as the wear rate with the speed, load and TiC amount has been explained on the basis of the hardness, the presence of transfer layer, the extent of cover provided by this layer to the underlying material and the ability to hold the thicker transfer layer. The nature of wear debris in the transfer layer i.e., loosely bound or well compacted has also been shown to affect the wear and friction. An increase in friction coefficient with increasing load and TiC has been attributed to the three body abrasion caused by the increasing amount of loose wear debris in the transfer layer. The addition of 4 wt.% TiC has been found to show the lowest wear rate under the conditions of loads and sliding speeds used in the present investigation.